

## A Theoretical Estimate of S-Wave Attenuation in Sediment

Gary. Mavko\*, Stanford University, Jack Dvorkin, Stanford University and Rock Solid Images, Joel Walls, Rock Solid Images

### ABSTRACT

Some of laboratory and field data (albeit very sparse) indicate that the S-wave attenuation in a sediment sample (a) weakly depends on water saturation and (b) approximately equals the P-wave attenuation at 100% water saturation. These observations are matched by our theoretical model. In this model we assume that (a) the S-wave inverse quality factor is related to the shear-modulus-versus-frequency dispersion by the same viscoelastic relation as the P-wave inverse quality factor (e.g., the standard linear solid) and (b) the shear-modulus-versus-frequency dispersion is linked to the compressional-modulus-versus-frequency dispersion.

To model the latter link, we assume that the reduction in the compressional modulus between the high-frequency and low-frequency limits is due to the introduction of a hypothetical set of aligned defects or flaws (e.g., cracks). Next we assume that the same set of defects is responsible for the reduction in the shear modulus between the high-frequency and low-frequency limits. Finally, by using Hudson's theory for cracked media we link the shear-modulus-versus-frequency dispersion to the compressional-modulus-versus-frequency dispersion and show that the proportionality coefficient between the two is a function of the P-to-S-wave velocity ratio (or Poisson's ratio). This coefficient falls between 0.5 and 3 for Poisson's ratio contained in the 0.25 to 0.35, typical for saturated earth materials.

### INTRODUCTION

In order to model the effects of intrinsic attenuation on seismic amplitude and to use these effects to help quantify lithology, porosity, and fluid saturation, it is necessary to measure or compute  $Q_p$  and  $Q_s$  from well log data. Since direct measurements of  $Q$  from sonic logs have been problematic, our approach is to use rock physics methods to estimate  $Q_p$  and  $Q_s$  from more conventional open-hole well log data. We have previously reported methods to 1) compute  $Q_p$  in partially water saturated rock (Dvorkin, et al, 2003), and 2) compute  $Q_p$  in fully water saturated rock (Dvorkin, Mavko, Walls, 2003). In this paper, we present a method to compute  $Q_s$  from well log data.

### S-WAVE ATTENUATION DATA

Laboratory measurements conducted at ultrasonic frequency on small rock plugs as well as in a lower frequency range using the resonant-bar technique on larger samples indicate that the S-wave inverse quality factor ( $Q_s^{-1}$ ) is weakly dependent on water saturation and is approximately the same as the inverse P-wave quality factor at full saturation ( $Q_s^{-1} \approx Q_p^{-1}$ ).

One example is the resonant-bar data from Murphy (1982) for Massillon sandstone (Figure 1). Lucet (1989) shows that the P-wave attenuation is close to S-wave attenuation in a limestone sample at ultrasonic frequency (Figure 2). However,  $Q_p^{-1}$  is larger than  $Q_s^{-1}$  at low (resonant-bar) frequency.

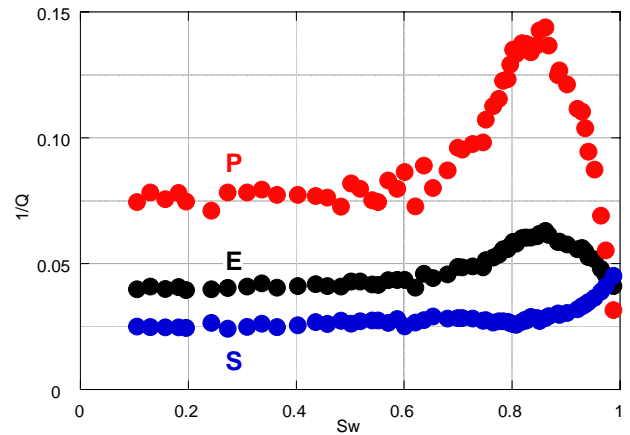


Figure 1. Resonance bar attenuation ( $1/Q$ ) data in Massillon sandstone of 23% porosity (Murphy, 1982). Frequency is between 300 and 600 Hz. The E- and S-wave data (black and blue, respectively) are measured while the P-wave inverse quality factor (red) is calculated from these data according to Winkler (1980).

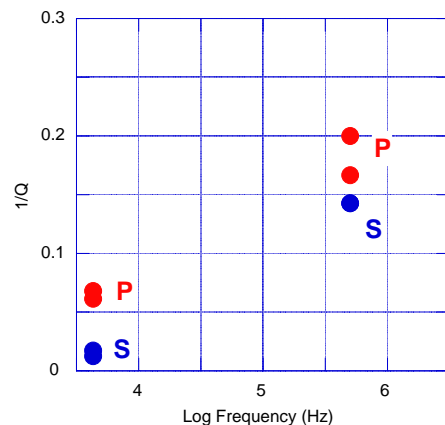


Figure 2.  $1/Q$  in a water-saturated limestone sample (Lucet, 1989).

## A Theoretical Estimate of S-Wave Attenuation in Sediment

Reliable field data for  $Q_p^{-1}$  and  $Q_s^{-1}$  is even more sparse than lab data. Useful results are due to Klimentos (1995) who shows from well log data that the S-wave attenuation is approximately the same as the P-wave attenuation in liquid-saturated sandstone while in gas-saturated intervals the P-wave attenuation is much larger than the S-wave attenuation (Figure 3).

Sun et al. (2000) compute the P- and S-wave attenuation from monopole sonic data. The reported  $Q_p^{-1}$  and  $Q_s^{-1}$  are essentially the same in low-shale-content interval but may be different in the shale.

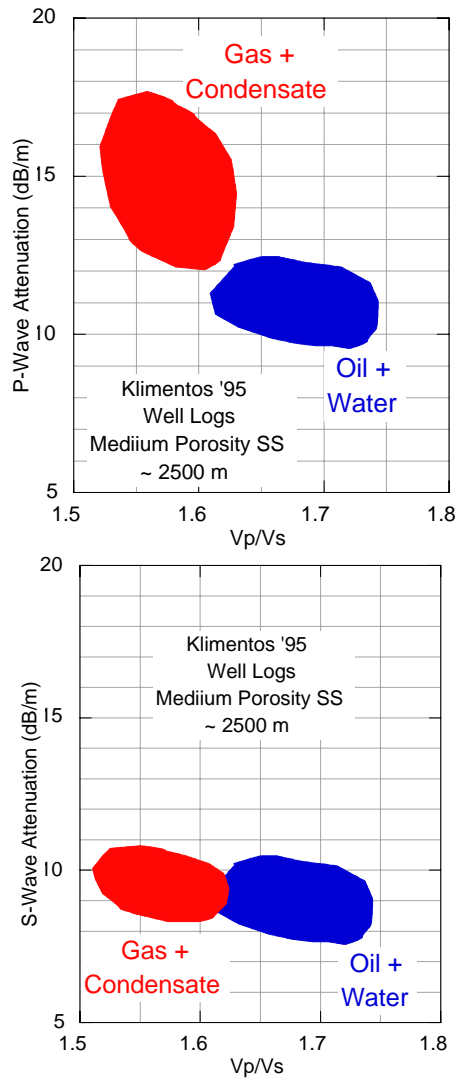


Figure 5. P and S-wave attenuation calculated from full-waveform sonic and dipole log data in medium-porosity sandstone with oil, water, gas, and gas condensate. After Klimentos (1995).

## S-WAVE ATTENUATION THEORY

### Attenuation and Modulus Dispersion

Our first assumption is that the inverse quality factor is related to the modulus-frequency dispersion by a viscoelastic causality relation, such as, e.g., for the Standard Linear Solid (Mavko et al., 1998):

$$2Q_p^{-1} = \frac{M_\infty - M_0}{\sqrt{M_0 M_\infty}}, \quad 2Q_s^{-1} = \frac{G_\infty - G_0}{\sqrt{G_0 G_\infty}}, \quad (1)$$

where  $M$  and  $G$  are the compressional and shear moduli, respectively, and the subscripts “ $\infty$ ” and “0” refer to the high- and low-frequency limits, respectively.

We will also assume that the S-wave attenuation is pore-fluid-independent and proceed with our analysis for fully-water-saturated porous sediment.

### Compressional Modulus Dispersion

We will use the Dvorkin and Mavko compressional modulus dispersion theory in wet sediment (Dvorkin and Mavko, 2005; Dvorkin and Uden, 2004). This theory states that the necessary condition for attenuation is elastic heterogeneity in rock. The low-frequency compressional modulus is calculated by theoretically substituting the pore fluid into the spatially averaged rock’s dry-frame modulus while the high-frequency modulus is the spatial average of the heterogeneous saturated-rock modulus. The difference between these two estimates may give rise to noticeable P-wave attenuation if elastic heterogeneity in rock is substantial.

### Link between P-wave and S-wave Modulus Dispersion

The physical basis for linking the compressional to shear modulus dispersion is the fact that there is a compressional element in shear deformation. Therefore, if a material includes viscoelastic elements that are responsible for the frequency-stiffening in the deformation-deformation mode, they will contribute to the stiffening in the pure-shear-deformation mode. Mavko and Jizba (1991) use this principle to estimate the contribution of soft crack-like pores containing liquid to the shear-modulus dispersion at ultrasonic frequency at the pore-scale (the microscopic squirt-flow). They show that the dispersion of the inverse shear modulus is about 4/15 of that in the inverse bulk modulus.

We will use the same principle. Specifically, we will assume that the reduction in the compressional modulus of wet rock between the high-frequency limit and low-frequency limit is due to the introduction of a hypothetical system of aligned defects (cracks) into the material. Next, we will adopt Hudson’s theory for cracked media (e.g., Mavko et al., 1998) to quantify these defects. Specifically, the reduction in the compressional modulus in the direction normal to the set of cracks is

## A Theoretical Estimate of S-Wave Attenuation in Sediment

$$M_\infty - M_0 = \Delta c_{11}^{\text{Hudson}}$$

$$\approx \varepsilon \frac{\lambda^2}{\mu} \frac{4(\lambda + 2\mu)}{3(\lambda + \mu)} \equiv \varepsilon \frac{4}{3} \frac{(M - 2G)^2}{G} \frac{M}{M - G}, \quad (2)$$

where  $\Delta c_{11}^{\text{Hudson}}$  is the change in the anisotropic stiffness component;  $\lambda$  and  $\mu$  are Lamé's constants of the background medium ( $\mu \equiv G$ ); and  $\varepsilon$  is the crack density -  $\varepsilon = 3\phi/(4\pi\alpha)$  - where  $\phi$  is the porosity and  $\alpha$  the aspect ratio. Assuming that  $M = \sqrt{M_0 M_\infty}$  we find from Equations (1) and (2) that

$$2Q_p^{-1} = \frac{M_\infty - M_0}{\sqrt{M_0 M_\infty}}$$

$$= \varepsilon \frac{4}{3} \frac{(M - 2G)^2}{G(M - G)} = \varepsilon \frac{4}{3} \frac{(M/G - 2)^2}{(M/G - 1)}. \quad (3)$$

The corresponding change in the shear modulus for the same set of aligned defects is given by the stiffness component  $c_{44}$ . The change in this component ( $\Delta c_{44}^{\text{Hudson}}$ ) due to the presence of cracks is

$$G_\infty - G_0 = \Delta c_{44}^{\text{Hudson}}$$

$$\approx \varepsilon \mu \frac{16(\lambda + 2\mu)}{3(3\lambda + 4\mu)} \equiv \varepsilon G \frac{16}{3} \frac{M}{3M - 2G}. \quad (4)$$

Assume next that  $G = \sqrt{G_0 G_\infty}$ . Then Equations (1) and (4) yield

$$2Q_s^{-1} = \frac{G_\infty - G_0}{\sqrt{G_0 G_\infty}} = \varepsilon \frac{16}{3} \frac{M}{3M - 2G}$$

$$= \varepsilon \frac{16}{3} \frac{M/G}{3M/G - 2}. \quad (5)$$

By combining Equations (3) and (5) we find

$$\frac{Q_p^{-1}}{Q_s^{-1}} = \frac{1}{4} \frac{(M/G - 2)^2 (3M/G - 2)}{(M/G - 1)(M/G)}, \quad (6)$$

where

$$\frac{M}{G} = \frac{2 - 2\nu}{1 - 2\nu} = \frac{V_p^2}{V_s^2}, \quad (7)$$

and  $\nu$  is Poisson's ratio.

In another variant of the same approach we may assume that the same set of defects is now randomly oriented in the material and thus does not introduce anisotropy. In this case the reduction in the isotropic shear modulus  $\Delta \mu^{\text{Hudson}}$  is

$$G_\infty - G_0 = \Delta \mu^{\text{Hudson}}$$

$$\approx \varepsilon \frac{2}{15} \mu \left[ \frac{16(\lambda + 2\mu)}{(3\lambda + 4\mu)} + \frac{8(\lambda + 2\mu)}{3(\lambda + \mu)} \right]. \quad (8)$$

In this case we find

$$2Q_s^{-1} = \frac{G_\infty - G_0}{\sqrt{G_0 G_\infty}}$$

$$= \varepsilon \frac{16}{15} \left[ \frac{2M/G}{(3M/G - 2)} + \frac{M/G}{3(M/G - 1)} \right] \quad (9)$$

and, as a result,

$$\frac{Q_p^{-1}}{Q_s^{-1}} = \frac{5}{4} \frac{(M/G - 2)^2}{(M/G - 1)} \left[ \frac{2M/G}{(3M/G - 2)} + \frac{M/G}{3(M/G - 1)} \right]. \quad (10)$$

Equations (6) and (10) present two versions for calculating  $Q_s^{-1}$  from  $Q_p^{-1}$ . It is important to remember that *in these calculations the wet-rock  $Q_p^{-1}$  has to be used*, i.e., in a hydrocarbon-saturated interval the original fluid has to be substituted for water and  $Q_p^{-1}$  calculated afterwards.

Finally, in the third variant of this approach we assume that the reduction in the compressional modulus is due to a set of randomly oriented isotropic defects and the same set of defects is responsible for the reduction in the shear modulus.

$$\frac{Q_p^{-1}}{Q_s^{-1}} = \frac{4}{3} \frac{1}{\lambda/\mu + 2} + \frac{5}{12} \frac{(3\lambda/\mu + 4)(3\lambda/\mu + 2)^2}{(\lambda/\mu + 2)(9\lambda/\mu + 10)}$$

$$= \frac{1}{M/G} \left[ \frac{4}{3} + \frac{5}{4} \frac{(M/G - 2/3)(M/G - 4/3)^2}{M/G - 8/9} \right]. \quad (11)$$

The  $Q_p^{-1}/Q_s^{-1}$  as given by Equations (6), (10), and (11) is plotted versus  $\nu$  in Figure 7. The three curves due to the three equations used differ from each other.

## A Theoretical Estimate of S-Wave Attenuation in Sediment

However, most importantly, they all predict  $Q_p^{-1}/Q_s^{-1}$  between 1 and 3 in the Poisson's ratio range between 0.30 and 0.35 which is typical for wet sediment. This predicted range of  $Q_p^{-1}/Q_s^{-1}$  matches the experimental observations.

### CONCLUSION

A simple theoretical model offered here relates the P-to-S inverse quality factor ratio to the Poisson's ratio of the background sediment. It relies on a large number of assumptions that are not necessarily honored in real rock. Yet, the attenuation ratio provided by the model is realistic and matches experimental observations. The main result is that in wet rock the P- and S-wave quality factors are approximately the same.

The theory essentially assumes that the waves propagate normal to the bedding or, more precisely, normal to the hypothetical defects responsible for the modulus dispersion. In more rigorous treatment of the problem, the direction of wave propagation needs to be taken into account or, at least its effects on the errors evaluated.

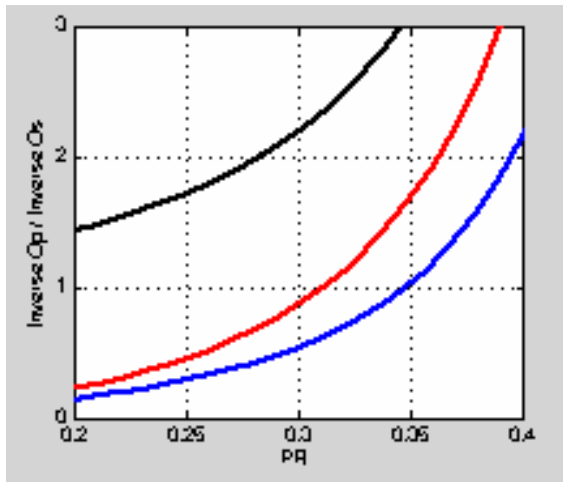


Figure 1. P-to-S inverse quality factor ratio versus Poisson's ratio. Blue curve (bottom) is from Equation (6), red curve (middle) is from Equation (10), and black curve (top) is from Equation (11).

### ACKNOWLEDGEMENTS

The work was supported by Rock Solid Images, the US Dept. of Energy (under contract DE-FC26-04NT42243), and Stanford Rock Physics Laboratory.

### REFERENCES

- Dvorkin, J., G. Mavko, J. Walls, M.T. Taner, N. Derzhi, 2003; Attenuation at Patchy Saturation – A Model, Proceedings of Annual EAGE Convention, Stavanger Norway, June 2-5.
- Dvorkin, J., and Uden, R., 2004, Seismic wave attenuation in a methane hydrate reservoir, *The Leading Edge*, 23, 730-734.

- Dvorkin, J., G. Mavko, and J. Walls, 2003; Seismic wave attenuation at full water saturation, Proceedings SEG Intl. Exposition and 73rd Annual Meeting, Dallas, TX, Oct 26-31.
- Klimentos, T., 1995, Attenuation of P- and S-waves as a method of distinguishing gas and condensate from oil and water, *Geophysics*, 60, 447-458.
- Lucet, N., 1989, Vitesse et atténuation des ondes élastiques soniques et ultrasoniques dans les roches sous pression de confinement, Ph.D. thesis, The University of Paris.
- Mavko, G., and Dvorkin, J., 2005, P-wave attenuation in reservoir and non-reservoir rock, Extended Abstract, EAGE 2005, Madrid.
- Mavko, G., and Jizba, D., 1991, Estimating grain-scale fluid effects on velocity dispersion in rocks, *Geophysics*, 56, 1940-1949.
- Mavko, G., Mukerji, T., and Dvorkin, J., 1998, *Rock Physics Handbook*, Cambridge University press.
- Murphy, W.F., 1982, Effects of microstructure and pore fluids on the acoustic properties of granular sedimentary materials, Ph.D. thesis, Stanford University.
- Sun, X., Tang, X., Cheng, C.H., and Frazer, L.N., 2000, P- and S-wave attenuation logs from monopole sonic data, *Geophysics*, 65, 755-765.
- Winkler, K.W., 1980, The effects of pore fluids and frictional sliding on seismic attenuation, Ph.D. thesis, Stanford University